Hyper- and Multispectral Imaging Systems– a Survey of Different Approaches at the Ilmenau University of Technology

M. Rosenberger, M. Correns, R. Fütterer, G. Linß, E. Manske, T. Fröhlich, A. Grewe, M. Hillenbrand, S. Sinzinger

Technische Universität Ilmenau

ABSTRACT

Hyperspectral imaging technologies and multispectral imaging technologies became more and more important for industrial measurement techniques, quality control and automation technologies. One unsolved problem is the fast and simultaneous image capturing of different spectral channels. The best approach up-to-date is known as push-broom scanner. On the Ilmenau University of Technology different methodologies are objective of the recent research as well as for the research in the future. The paper gives a survey about the different approaches. The paper starts with a system which deals with the principle of FTIR Spectroscopy, which needs a mathematic transformation to deliver spectral image data. In the following two chapters a confocal approach using tunable optical elements based on Alvarez Lohmann lenses will be presented. The paper ends with a multispectral system operating with different color filters.

Index Terms *–Hyperspectral imaging, Multispectral imaging, Hyperspectral FTIR Spectroscopy, Chromatic confocal spectral sensing, Alvarez Lohmann Lens System, Discrete Filter Elements;*

1. INTRODUCTION

During the recent years the department *Optical Engineering*, the *Institute of Process Measurement and Sensor Technology* and the department *Quality Assurance and Industrial Image Processing* were working on different technologies to capture spectral images. The objectives of these research activities are the increase of sampling speed, the increase of spectral resolution as well as the increase of spatial information of the device under test. In this first common paper the investigations into the different capture technologies are presented.

2. Hyperspectral imaging on the basis of FFT-spectroscopy

In the field of spectroscopy, two very efficient methods have become well-established: grid spectroscopy and the Fourier-Transform-Spectroscopy (frequently called FTIR-spectroscopy in the infrared wavelength range). Hyperspectral imaging on the basis of diffraction gratings only allows linear sampling. The recent development of the Fourier-Transform-Spectroscopy (FTS) especially in the infrared wavelength (FTIRS) range makes this technology an important method in the fields of environmental just as analytical metrology. However, one disadvantage is the dimensions of these devices. For FTIR-spectroscopy, sophisticated interferometers equipped with highly accurate and precise mirrors have to be used.

Today, the detection of nanoplasmonic nanoparticles has become a field of application for hyperspectral imaging techniques based on FTIR. Some first developments in this field have already been presented [1, 2]. However, a major disadvantage of these approaches is that for recording the interferograms, mostly piezo translators with a measuring range of 16µm [1] to 30µm [2] are employed without any additional (interferometric) measuring system. In order to keep the number of measurements low, only 80 images are captured, which corresponds to a wavelength resolution of about 20µm [1]. Also, in order to minimize the efforts involved in the parallel Fourier transformation, the image regions to be considered are selected through image processing. Thus, only relatively few FFTs are recorded, which greatly reduces the computational efforts.

The Institute of Process Measurement and Sensor Technology (IPMS) can look back on longstanding expertise in the development of nanopositioning and nanomeasuring machines. High-precision drive control, miniaturized fibre-coupled laser interferometers as well as optical probes like the massively parallel white-light interference microscopy [3] were in the focus of the most recent research work.

By combining these techniques, some first bases of hyperspectral imaging systems have been developed at the IPMS. For creating a general approach of „hyperspectral imaging“, a set-up was designed which allows a high-precision, equidistant and massively parallel interferogram recording (Fig. 1).

Due to the fact that the spectral range includes the visible up to the near infrared, no special optics or photoelectric elements are required. The displacement of the movable mirror is measured by means of a fibre-coupled miniature interferometer with a resolution of 80 pm [SIOS plane mirror]. The optical path of the laser interferometer is combined with the optical path of the spectrometer as it is also practiced in the case of single-ray FFT-spectrometers. However, the advantage lies in the compact design of the fibre-coupled interferometer.

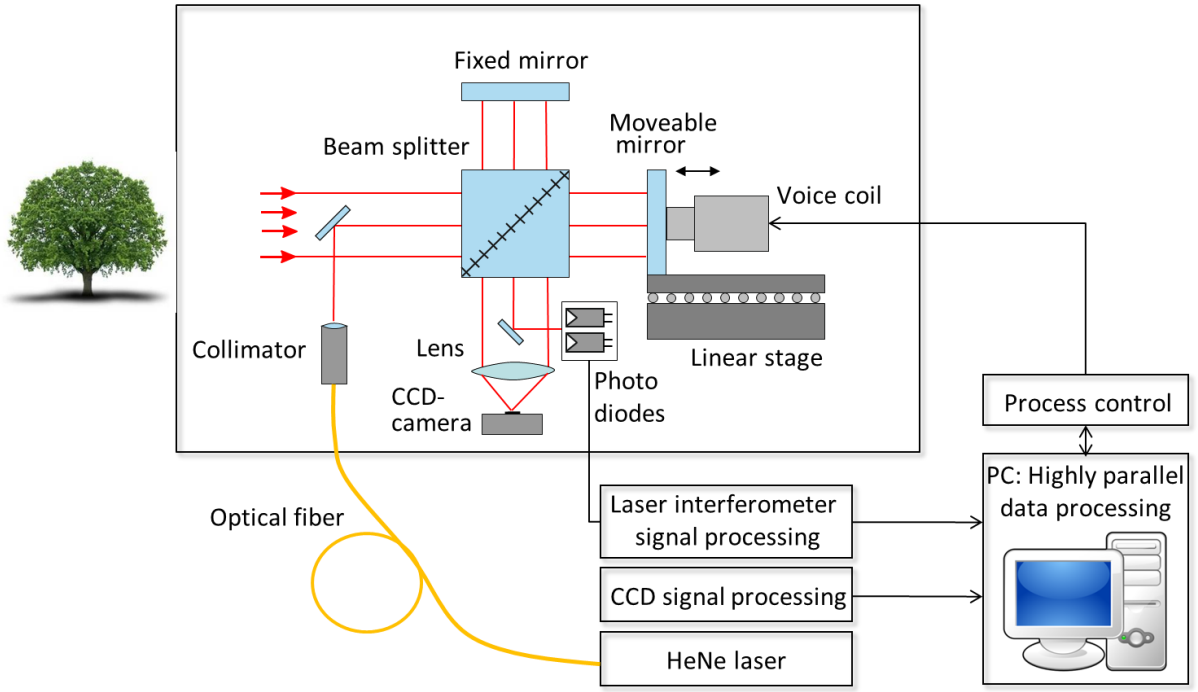

Figure 1: Concept of hyperspectral imaging arrangement

The interesting scene can be imaged onto the CCD-camera by means of a photographic lens. Figure 2 shows the example of such a white-light interferogram. However, this approach can also be applied to the hyperspectral imaging of microscopic objects. By means of voice-coil-

drives operating in a closed-loop mode with the interferometers, image stacks of 1024 or more single shots can be captured at nanometer resolution over hundreds of micrometers [5]. Thus, a spectral resolution of clearly below one nanometre is achieved. Today, depending on the type of CCD-camera, the single images can contain 1 megapixel up to 6 megapixels (or even more).

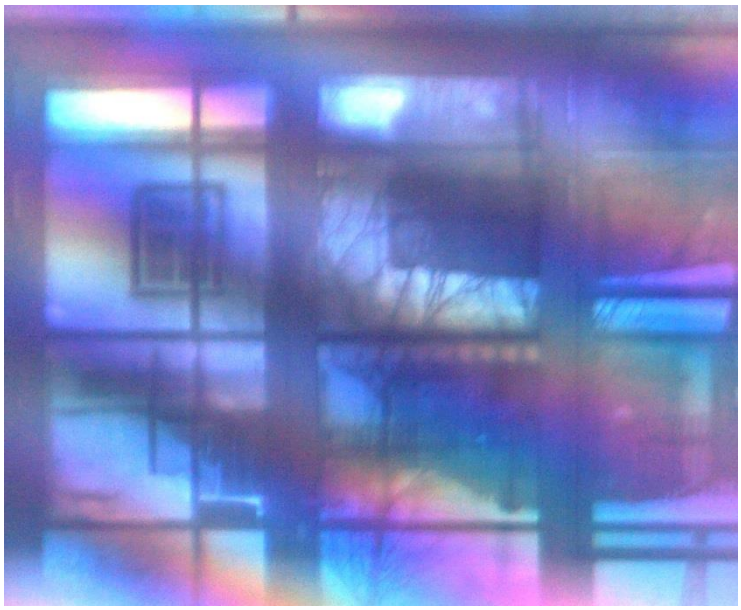

Figure 2: Interferometric image of a landscape. This leads to the necessity of massively parallel information processing which includes phase correction, apodisation, zero-filling just as FFT and the subsequent output or visualization of the spectral image data.

The storage and numerical computation of 1024 images with 1 million pixels are possible with current office PCs. The images have roughly 2^{20} times 3 byte for the colours, which is about 3 Mbyte and thus, 3 Gbyte for all 2^{10} images. For computing the FFT of all vertical pixel stacks with 1024 elements, we have used MATLAB. If we use single floating point numbers and the internal vectorization (instead of loops over the pixels), we will get the computing time for calculating the phase and the amplitude depending on the number of pixels. Then we take the mean value and the standard deviation for ten repetitions (cf. Fig. 3 for the code used, and Table 1 for the results). For 2^{19} pixel stacks, which are 0.5 million, we obtain a computing time of 1.3 seconds. For 1 million, we obtain much more than double time because of the memory limitations. The input matrix of 4 Gbyte would, of course, fit into the memory of 16 Gbyte, but together with the complex result the system needs to swap to the hard disk. Furthermore, this leads to a much higher standard deviation of the measured computation time. In summary, for problems not fitting into the main memory completely, it would be faster to split the problem into two or more computational stages. Thus, it would be possible to transform 1024 images at megapixel resolution in less than 3 seconds using the CPU.

# of pixel stacks	2^{15}	2^{16}	2^{17}	2^{18}	2^{19}	2^{20}
Mean time in s	0.084	0.167	0.333	0.665	1.33	75.3
Std in s	0.005	0.007	0.012	0.025	0.05	30.9

Table 1: Computing time for different input matrix sizes

```
EE=[15 16 17 18 19 20];
timeX=zeros(10,length(EE));
for ee=1:length(EE);
      x=randn(1024,2^EE(ee),'single');
      for ii=1:10,
            tic;
            y=fft(x);
            timeX(ii,ee)=toc
      end
end
[EE;mean(timeX);std(timeX);]
```

Figure 3: MATLAB code used to benchmark CPU results shown in Table 1

We have tried CUDA calculations with single floating point and have found a much lower memory limit because problems bigger than 2^{16} pixel stacks would not fit in our CUDA graphics card. For 2^{15} and 2^{16} we have achieved a computing time of 0.009 s and 0.025 s, resp., which is seven times faster than the CPU.

```
EE=[14 15 16];
timeX=zeros(10,length(EE));
for ee=1:length(EE);
x=gpuArray(randn(1024,2^EE(ee),'single'));
for ii=1:10,
            tic;
            for kk=1:100, y=fft(x);x=y; end,
            timeX(ii,ee)=toc
      end
end
[EE;mean(timeX)/100;std(timeX)/100;]
```

Figure 4: MATLAB code used to benchmark GPU results

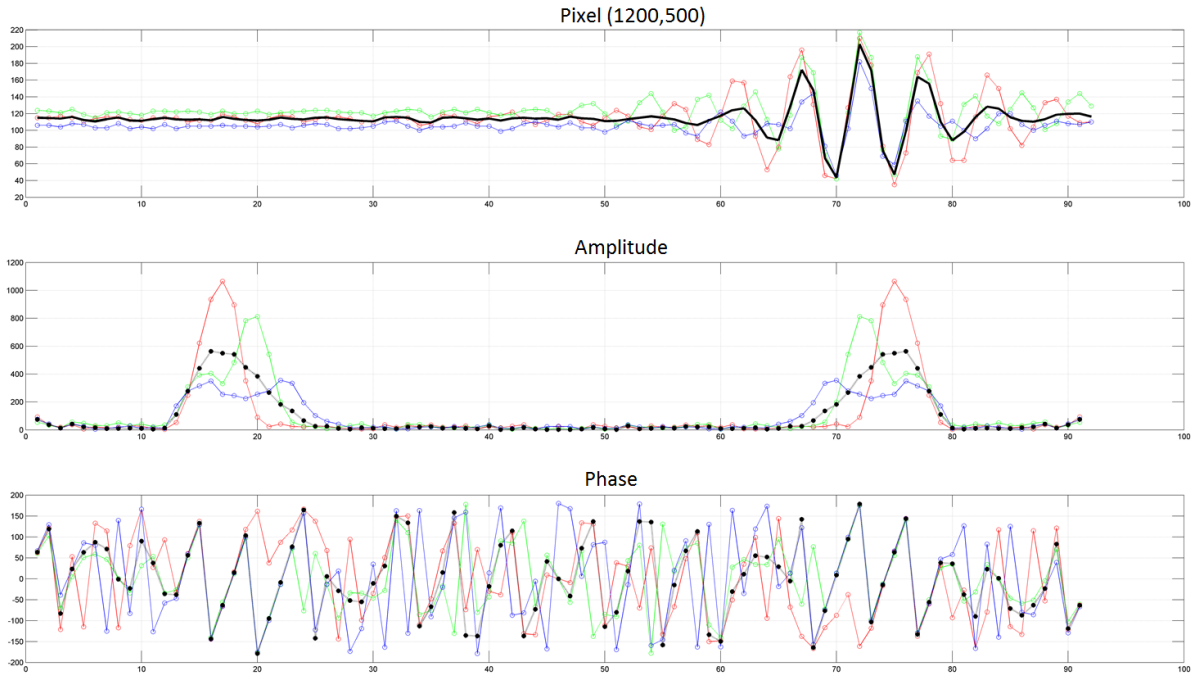

Figure 5: RGB and intensity over z height for one pixel and amplitude and phase of the FFT calculation

With the aid of our nanopositioning and nanomeasuring machine and a white light interference microscope we captured a height scan of a special Si-structure with 1 million pixel in parallel. Exemplarily, in Figure 5 the intensity of the three colour channels of the CCD camera and over the z heigt of one pixel measured at a measuring object (Fig. 6) and the amplitude and phase of the FFT calculation are presented. The spectral information depending on the spectra of the illumination and of the spectral properties of the surface can be received especially from the phase information of the FFT. In Figure 6, left sight, the RGB image of the surface of the measuring object including the white light interference at one height position can be seen. On the right sight the calculated height profile as one result of the parallel FFT calculation of the surface is shown. In the same way the spectral information of every pixel is incorporated in the FFT and can be extracted.

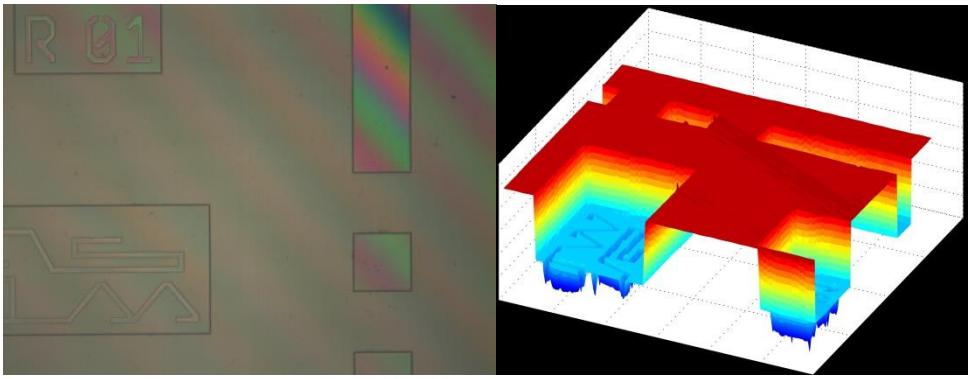

Figure 6: RGB image detail and calculated height profile

3. CHROMATIC CONFOCAL SPECTRAL SENSING

In chromatic confocal sensor systems a small aperture, a so called pinhole, is imaged by an optical system. The longitudinal chromatic aberration of the optical system is used to separate the spectral components of the incident light along the optical axis. Optical systems with a specially extended longitudinal chromatic aberration are called hyperchromats [6, 7]. The hyperchromat generates multiple images of the pinhole along the optical axis, one for each wavelength. Hence at an arbitrary plane in image space only one wavelength is ideally focused. A second pinhole at such a plane, as shown in figure 7a, permits only the light of the ideally focused wavelength to pass unattenuated. All other wavelengths are out of focus and a major portion of their intensity is shut off by the pinhole. For each position of the pinhole along the optical axis a different wavelength produces an intensity maximum behind the pinhole. Hence with knowledge of the sensors wavelength-distance correlation the whole spectrum of the incident light can be analyzed by moving the pinhole along the optical axis while recording the intensity behind the pinhole, see figure 7b.

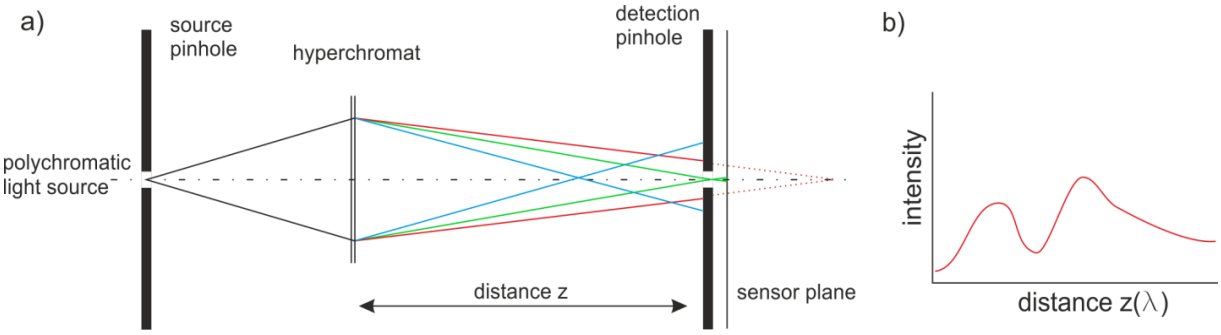

Figure 7: a) chromatic confocal setup with movable detection pinhole; b) exemplary intensity – distance correlation of a confocal spectrometer system

This confocal chromatic spectrometer is enhanced into a hyperspectral imager when multiple pinholes are imaged parallel by telecentric hyperchromatic optics [8-10]. The scenery to be tested is imaged on the first pinhole array. Each pinhole is used to analyze the spectrum at a different spatial coordinate. The intensity behind the detector pinhole array is measured with an array sensor like a CCD. Here the axial scan is especially delicate since the whole detector array has to be moved together with the detection pinhole array and the necessary electronics. A possibility to avoid the movement of the detector unit is the employment of tunable optical elements to alternate the focal length of the optical system.

3.1 Parallelization with tunable optical elements

Tunable optical elements are optical subsystems, which actively alternate the properties of an optical system, in most cases the focal length. Classic examples are zoom lenses with axially moving lens groups, but recently a variety of different principles have been developed [11,12]. For the development of a compact hyperspectral imager we pursued two different approaches. In cooperation the Department of Microsystems Engineering at the University of Freiburg and the department Optical Engineering at Ilmenau University of Technology developed a chromatic confocal hyperspectral imaging system incorporating a hybrid diffractive-refractive fluidic lens [13]. A second approach, exploited by the department Optical Engineering in Ilmenau, was the use of hyperspectral Alvarez-Lohmann lenses. These freeform elements feature a variable focal length dependent on their lateral displacement. The Alvarez-Lohmann system is presented in this paper.

4. ALVAREZ LOHMANN LENS SYSTEM

Alvarez-Lohmann lenses consist of two cubic phase plates which are orientated in a way that they form a plane-parallel plate. However by a lateral displacement of the plates relative to each other, they generate a parabolic wavefront much like a lens. Since the curvature of the resulting wavefront is proportional to the amount of displacement, they act as varifocal elements [14, 15]. We combined diffractive Alvarez-Lohmann lenses (DOEs) with refractive aspheres to form the hybrid tunable hyperchromatic lens shown in figure 8. To minimize aberrations, the Alvarez-Lohmann DOEs are placed near the systems aperture.

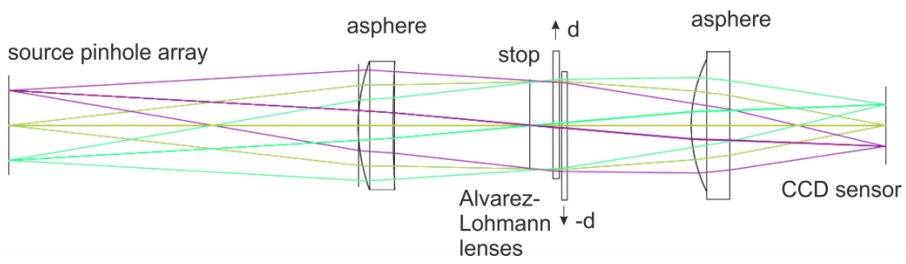

Figure 8: Optical layout of the hybrid Alvarez Lohmann lens system. The source pinhole array is located at the image plane of an additional photo lens.

The Alvarez-Lohmann lens model is based on a thin element approximation. To compensate for the errors which are generated when transferring this model to real elements, we used higher order polynomial descriptions up to the 7th order to optimize the phase plates [16]. Design goals are the imaging quality, the longitudinal chromatic aberration as well as the numerical aperture of the system, which is proportional to the spectral resolution [8, 17].
Using a two-step lithography / ICP-RIE process the diffractive elements were realized in SiO2 as 4 level DOEs. A maximum phase gradient of 240 waves/mm was designed to meet the minimal feature size of 1µm.
The optimized Alvarez-Lohmann lenses realize the extended chromatic aberration with a total longitudinal aberration of 4.8 mm for a spectral range between 450 and 750 nm. By a lateral shift of the plates, the focal length of the system is tuned to sequentially image the spectral components of the incident light at the detection pinhole plane. The maximum field angle of the system is ±4.6° and the spectral resolution of the on axis point is below 25 nm FWHM. A test measurement of a white light source is shown in figure 9.

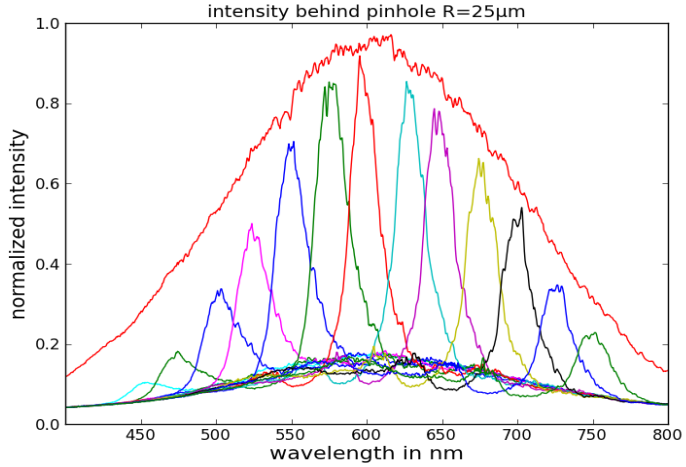

Figure 9: The spectrum of a white light source is scanned with the Alvarez-Lohmann system. In this measurement the signal behind the on axis pinhole is analyzed with a spectrometer.

5. MULTISPECTRAL ACQUISITION USING DISCRETE FILTER ELEMENTS

Besides the hyperspectral imaging technologies, for some applications also multispectral camera systems are well suited. Therefore a set of filters with different wavelength ranges were positioned in front of a CMOS or a CCD sensor. If the filter covers the full image sensor area, the sensor has to be shuttered. In the most systems a circular filter system is used. The fast synchronization is essential to achieve a fast capturing process. With a high speed sensor up to 40fps with full spectral resolution were captured in [18]. The actual design of the filter-

wheel system carries twelve different filters with a span of 50 nm beginning at 400 nm illustrated in figure 10.

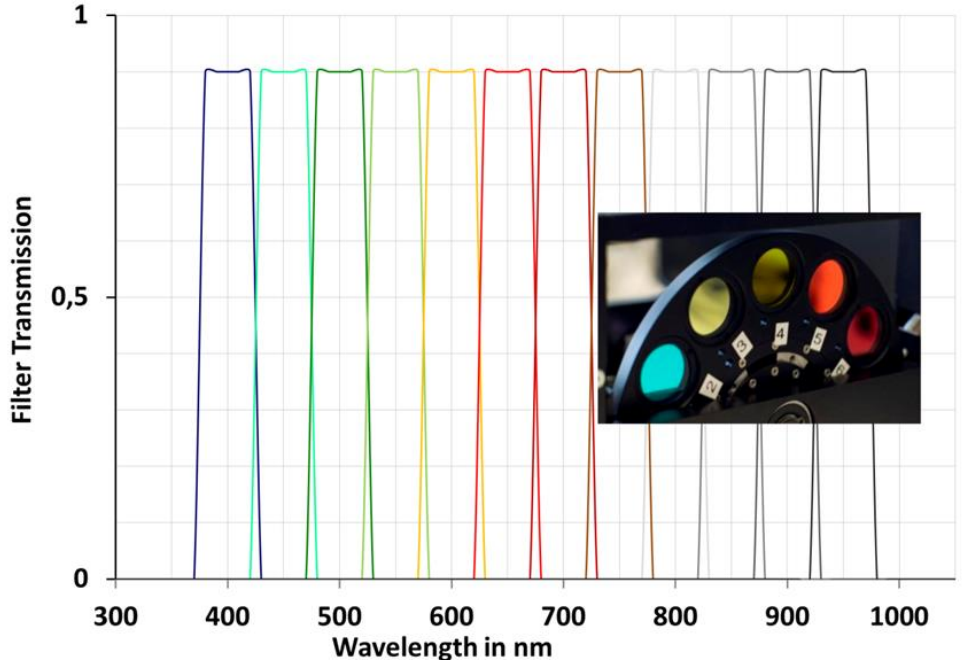

Figure 10 :Filter wavelength distribution with hard coded metal interference filter, assembled filter-wheel inside the camera in the left upper corner

A big advantage of these systems is the full space resolution of the images. Due to the accurate wavelength calibrations of the filter sets the captured images are also well-adjusted in the wavelength range.
For the correct image acquisition the individual filters must completely cover the sensor surface during the integration time of the sensor. Beyond that, boundary regions and the filter mounting plate must not cover the sensor, since this leads to vignetting. Therefore filter positioning and image acquisition must be synchronized.
Two possibilities are conceivable. On the one hand to adapt the frame rate as functions of engine speed and filter position. In this case, the image acquisition can be adjusted by an asynchronous reset, each time the middle filter position match the sensor position. Disadvantage here is that the maximum frame rate of the sensor is not utilized. A further possibility for the synchronization offers the dynamic regulation of the engine speed, with constant image frequency of the sensor. Thus the maximum frame rate can be used, however the control expenditure is larger. For the accurate synchronization the controlled variables engine speed, filter position and image frequency must be determined in real time. For the determination of the current filter wheel position two reflected-light barriers and a biunique coding were implemented on the filter wheel [S1 and S2 in figure 11].
The engine speed is determined directly over the motor control. The current number of revolutions of the brushless DC motor is supervised by a Hall sensor and can be queried at any time. Accordingly a target number of revolutions can be specified over the motor control. Communication is serial RS232 [S3 in figure 11].
The synchronization signals of the camera represent the frame and the line valid signal [S4 and S5 in figure 11]. On the other hand an asynchronous image acquisition can be initiated over the trigger line [S8 in figure 11].
All measuring and control quantities are parallel supervised and regulated by the FPGA in real time. Both initially described control methods are to be examined and implemented. For the filter wheel camera a combination of both methods is conceivable, in order to adjust the

mechanical start-up phase of the filter wheel and to synchronize later on maximum frame rate [18].

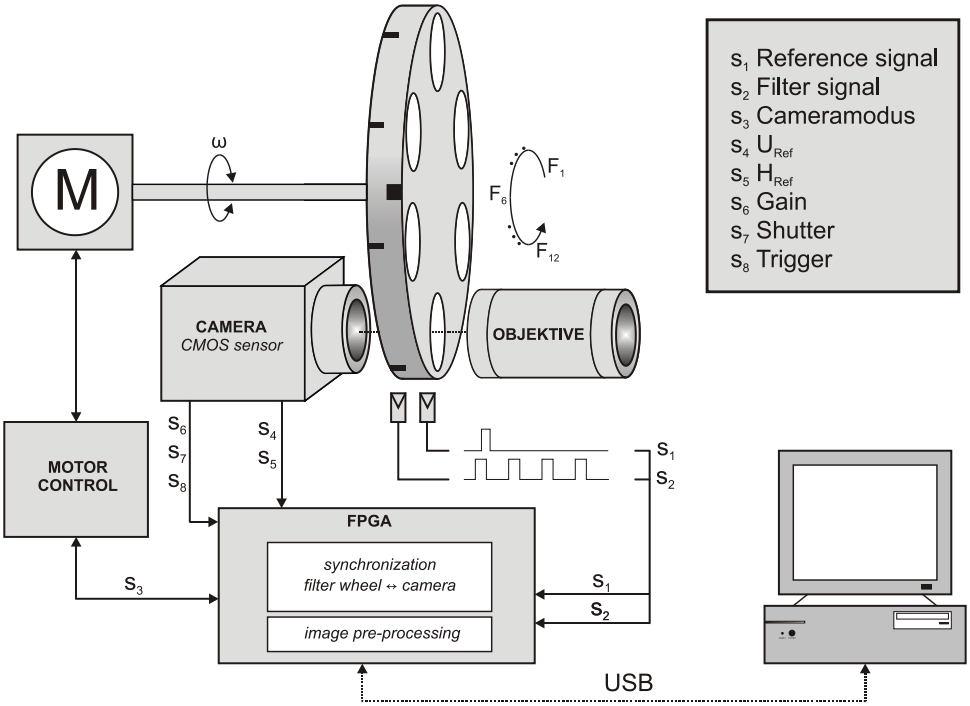

Figure 11: Schematics of the filter-wheel system

For all the signals which were transmitted into the FPGA a live tagging of the images was realized. If the FPGA detect a new filter it writes the filter number in the black shoulder of the image. Therefore the pixel-stream was manipulated in this region of the image without interruption. With this little tag the image processing unit got the information which filter wavelength is applied to the current image. Furthermore with this information an asynchronous live cam viewer can reconstruct and display the multispectral cube.
But nevertheless there are also challenges that have to be fixed. Actual improvements concerning the chromatic aberrations which lead to blurred images are part of the future work.

6. CONCLUSION

The Institute of Process Measurement and Sensor Technology presented in this paper some approaches concerning the further development of hyperspectral image processing on the basis of FFT-spectroscopy in the visible and near infrared range. High-precision drive control, miniaturized fibre-coupled laser interferometers as well as massively parallel CCD-image processing combined with high-throughput signal processing constitute an important basis. Very efficient computing systems allow the spectral measurement data to be calculated quickly at one and the same time. By combining these techniques, some first bases for hyperspectral imaging systems have been developed at the Institute of Process Measurement and Sensor Technology. The department Optical Engineering presented a confocal approach to hyperspectral imaging using tunable optical elements. A hybrid system based on Alvarez-Lohmann lenses is presented. To meet the requirements of a hyperspectral imaging system, the Alvarez-Lohmann lenses were enhanced by higher polynomial term up to the 7th order. The system was fabricated and first characterizations were executed. The department Quality Assurance and Industrial Image Processing shows the realization of a multi spectral imaging system based on a filter wheel system. Therewith it is possible to capture images with twelve

channels in the VIS and the NIR range of the electromagnetic spectrum. The multispectral imager delivers valuable information for industrial quality assurance applications.

ACKNOWLEGDEMENTS

This work was supported by the federal ministry of education and research (BMBF) in the Project Qualimess (03IP709) and OpMiSen (16SV5575K).

REFERENCES

Literature:

[1] T.-Y. Tseng, P.-J. Lai, K.-B. Sung: High-throughput detection of immobilized plasmonic nanoparticles by a hyperspectral imaging system based on Fourier transform spectrometry, Optics express 2011, 19, 2, 1291–300

[2] E. Manske; G. Jäger; T. Hausotte; R. Füßl: Recent developments and challenges of nanopositioning and nanomeasuring technology. In: Measurement Science and Technology, Vol. 23, 074001 (10pp), 2012

[3] N. Jahr: Herstellung und Charakterisierung neuartiger Hybridnanostrukturen für bioanalytische Anwendungen. Dissertation TU Ilmenau, 2014, 113 S.

[4] SIOS: Miniaturinterferometer mit Planspiegelreflektor. http://www.sios.de/DEUTSCH/PRODUKTE/SP_dt_2014.pdf. 09.07.2014

[5] T. Machleidt; E. Sparrer; E. Manske; D. Kapusi; K.-H. Franke: Area-based optical 2.5D sensors of a nanopositioning and nanomeasuring machine. In: Measurement Science and Technology, Vol. 23, 074010 (6pp), 2012

[6] G. Molesini, G. Pedrini, P. Poggi, and F. Quercioli; “Focus-wavelength encoded optical profilometer”; In: Optics Communications 49, 229-233 (1984).

[7] R. Leach, Optical Measurement of Surface Topography (Springer, Berlin Heidelberg, 2011)

[8] M. Hillenbrand, A. Grewe, M. Bichra, B. Mitschunas, R. Kirner, R. Weiß, and S. Sinzinger; “Chromatic information coding in optical systems for hyperspectral imaging and chromatic confocal sensing”; In: Proc SPIE 8550, 85500D (2012).

[9] M. Hillenbrand, A. Grewe, M. Bichra, R. Kleindienst, L. Lorenz, R. Kirner, R. Weiß, and S. Sinzinger; “Parallelized chromatic confocal sensor systems”; In: Proc SPIE 8788, 87880V (2013).

[10] K. Körner; „Verfahren und Anordnung zur schnellen, ortsaufgelösten, flächigen, spektroskopischen Analyse, bzw. zum Spectral Imaging oder zur 3D-Erfassung mittels Spektroskopie“; Patent DE102006007172 B4 , 2006

[11] A. Werber and H. Zappe, “Tunable microfluidic microlenses”; In: Appl. Opt. 44, 3238–3245 (2005).

[12] Ch. Song, N.T. Nguyen, A.K. ASundi and S.H. Tan; “Tunable micro-optofluidic prism based on liquid-core liquid-cladding configuration”; In: Optics Letters Vol. 35, No. 3 2010

[13] P.H. Cu-Nguyen, A. Grewe, M. Hillenbrand, S. Sinzinger, A. Seifert and H. Zappe; „Tunable hyperchromatic lens system for confocal hyperspectral sensing“, In: Optics Express Vol. 21, 2013

[14] L. W. Alvarez; “Two-Element variable-power spherical lens”; US Patent 3,305,294 (1967).

[15] A. Lohmann and D. Paris; “Variable Fresnel Zone Pattern”; Applied optics 6, 1567-1570 (1967).

[16] Grewe, Hillenbrand, Endrödy, Hoffmann, and Sinzinger; “Advanced phase plates for confocal hyperspectral imaging systems”; In: OSA Optics and Photonics Congress: Imaging and Applied Optics, Arlington, USA, 2013

[17] M. Hillenbrand, B. Mitschunas, C. Wenzel, A. Grewe, X. Ma, P. Feßer, M. Bichra, and S. Sinzinger; “Hybrid hyperchromats for chromatic confocal sensor systems”; In: Advanced Optical Technologies 1, 187-194 (2012).

[18] Preißler M., Rosenberger M., Correns M., Schellhorn M., Linss G.: „Investigation on a modular high speed multispectral camera“ - In: Proceedings of the 20th IMEKO TC2 Symposium on Photonics in Measurement (2011), ISBN 978-3-8440-0058-0,

CONTACTS

Dr.-Ing. M. Rosenberger maik.rosenberger@tu-ilmenau.de
Prof. Dr.-Ing. habil. E. Manske eberhardt.manske@tu-ilmenau.de
Dipl. -Ing. A. Grewe adrian.grewe@tu-ilmenau.de

